Applied Engineering
2022; 6(2): 30-38
http://www.sciencepublishinggroup.com/j/ae
doi: 10.11648/j.ae.20220602.11

Influence of Curvature and Torsion on the Friction Factor of Helical Pipe Flow

Anup Kumer Datta[1, *], Marzia Yesmin[1], Anindita Paul[2], Md. Sifuzzaman[3]

[1]Department of Mathematics and Statistics, Bangladesh University of Textiles, Dhaka, Bangladesh

[2]Department of Mathematical and Physical Sciences, East West University, Dhaka, Bangladesh

[3]Department of Computer Science and Engineering, Dhaka International University, Dhaka, Bangladesh

Email address:

akd_math_02@yahoo.com (A. K. Datta)

[*]Corresponding author

To cite this article:

Anup Kumer Datta, Marzia Yesmin, Anindita Paul, Md. Sifuzzaman. Influence of Curvature and Torsion on the Friction Factor of Helical Pipe Flow. *Applied Engineering*. Vol. 6, No. 2, 2022, pp. 30-38. doi: 10.11648/j.ae.20220602.11

Received: June 24, 2022; **Accepted**: July 25, 2022; **Published**: August 5, 2022

Abstract: Three-dimensional (3D) direct numerical simulations (DNS) were used to investigate the friction factor of helical pipe for an extensive range of curvature, torsion parameter, and the Reynolds number. In order to explore the friction factor of the helical pipe, performed steady solutions by steady 3D calculations, where the friction factor was calculated in the appearance of well-developed flow regions, being in good agreement with the experimental data. It is found that the tendency of the friction factor of the helical pipe sharply upturns when weak rotational forces due to the pitch-induced torsion are provided then reduces after taking a global maximum value of the friction factor, and finally slowly approaches that of a straight pipe when strong rotational forces gradually appears. After a comprehensive analysis of the ongoing exploration over the parametric ranges the existence of global maximum peak of the friction factor obtained whatever the values of curvature and Reynolds number. It is interesting that the present paper explored the bound of torsion parameter where the friction factor of the helical pipe is applicable to the toroidal pipe and straight pipe. For finite values of curvature over the extensive ranges, there occurs an interaction between Reynolds number and rotational forces, when various interesting phenomena arises, which reveals the crucial importance of the curvature and torsion parameter in the dynamics of helical pipe flow.

Keywords: Helical Circular Pipe, Curvature Effect, Torsion Effect, Three-Dimensional Numerical Simulation, Steady Solution

1. Introduction

Fluid flow in helical pipes has an extensive application in various industries: chemical, biomedical, mechanical, agriculture, and also applied in a wide range of processes: water supply, drainage, separation, and reaction. The existence of a complex secondary flow in the surface perpendicular to the principle flow is one of the vital structures in helical pipe. When fluid flow enters a toroidal pipe (zero pitch-induced torsion), the outer wall of the curved pipe acts like a complication, and pressure is built up on the outer wall. Accordingly, the fluid near the inner wall is faster than the fluid near the outer wall. One of the principal characteristics in a toroidal pipe is that the centrifugal force is formed by curvature and the unevenness in the centrifugal force on a cross-section causes a secondary flow, indicated by the strength of the cross sectional average fluid velocity. By the centrifugal force, the fluid located near the inner wall is moved toward the outer wall through the core region. A typical secondary flow is formed as a symmetric two-vortex pattern, where one appears near the top wall and the other near the bottom wall, where there is no torsion effect. However, the symmetric two-vortex pattern changes into asymmetric and finally one cell pattern due to the influence of torsion, where yields the dissimilar flow structure from the toroidal pipe. With the influence of curvature and torsion in the helical pipe, the internal flow structure is changed.

Yanase et al. [1] performed the dual solution of a helical pipe with a zero pitch in the steady laminar flow region,

numerically. They implement the spectral method for numerical calculations, where the flow is uniform in the stream-wise direction (two-dimensionality) for the helical pipe with a zero pitch. They proposed a correlation that can estimate the friction factor of a helical pipe with a zero pitch for the extensive range of Dean numbers.

Liu and Masliyah [2] numerically studied the friction factor of the helical pipe in the laminar flow region for rationally enormous pitches and limited range of curvature, where they assumed that the flow is uniform in the z-direction. They obtained the scenario of the friction factor as a task of enormous pitches and for limited curvature. They found that the highest value of friction factor from that a helical pipe with a zero pitch for numerous Dean numbers except for low Dean numbers.

Yamamoto et al. [3] investigated the friction factor of helical pipe for an extensive range of β and $0.01 \leq \delta \leq 0.1$, experimentally. They obtained the trend of the friction factor that lies upstairs on the straight pipe for the highest β. where it declines as β rises from the lowest value of β.

Based on the experimental data [4], Yamamoto et al. conducted the neutral curve of the instability of helical pipe for finite value of torsion parameter using the spectral method. It is to be noted that obtained critical Reynolds numbers rationally good agreement with the experiment results.

Cioncolini and Santini [5] performed the friction factor in the helical pipe, experimentally. They determined the critical point of laminar to turbulent transition with the influences of curvature and insignificant torsion (toroidal pipe) and the results authenticated by Ito's correlation formula [7] for the extensive range of curvature.

Xiao et al. [6], Yu et al. [7] performed the physical appearance of pressure drop and heat transfer for multi-phase flow in experimentally and numerically by the effect of shape of helical pipe and flow parameters.

Datta et al. [8] numerically conducted the turbulent flow in a helical pipe with the experimental data. Based on the experimental data, they explored the friction factor of the helical pipe for low torsion and found the relevant turbulence model that can estimate the friction factor. Datta et al. [9-10] also explored the friction factor and average Nusselt number of helical pipe flow by 3D DNS.

Garcia et al. [11] conducted the fanning friction factor through several helical pipes experimentally. They developed a correlation for laminar- turbulent flow that can estimate the friction factor of a helical pipe as a task of cross sectional average velocity with low pitch induce torsion. Owing to outstanding analysis, the friction factor of helical pipe has been disclosed by Patil [12], Solanki and Kumar [13].

Recently, as for the helical pipe flow, Datta *et al*. [14] found the critical Reynolds numbers of the laminar to turbulent transition by 3D DNS for an extensive range of β, which is rationally agreed with 2D spectral study obtained by Yamamoto et al. [4] for $\beta \leq 1.4$. However, for $\beta \leq 1.6$, the critical Reynolds numbers obtained by present DNS were much lower than those by Yamamoto et al. [4] and disturbances with 3D vortical structures developed slightly above the critical state in the form of a travelling-wave solution.

Even though there are many researches have been conducted friction factor with finite pitch, there exists no numerical investigation due to the combined effects of strong centrifugal force due to δ and swirl motion owing to β, where comparison of the numerical results with the experimental results have been executed to the authors' knowledge. It is worth mentioning that the friction factors of the helical pipe in the laminar region are performed comprehensively by 3D DNS due to the combined effects of an extensive range of curvature, torsion with the Reynolds number, which is the first finding to the authors' knowledge.

In the existing study, OpenFOAM to analyze the friction factor of the helical pipe by an orthogonal coordinate system, where conducted 3D DNS with good accuracy, using the similar manner of Datta et al. [8-10, 14], which is the key concentration of this study. To verify the numerical accuracy, associated the friction factor by present DNS with the experimental data obtained by Yamamoto et al. [3] for several curvatures. In the parametric analysis of torsion, and curvature, the present paper explore numerically the friction factor of the helical pipe, unequivocally, which is another new objective of the current study. To investigate the friction factor due the effect of finite torsion by performing the variation of the curvature for increasing the Reynolds number.

2. Numerical Simulation

2.1. Geometry of the Helical Pipe

A model simulation domain for a uniform axial flow in a helical pipe is shown in Figure 1. The domain consists the internal diameter with length $2a$, which enters a helical pipe section that forms a circular arc, and $2\pi h$ the one pitch length of the helical pipe. A broken line represents the center line of the helical pipe and R is the distance of the center line from the axis of the whole structure indicated by a long and little dashed line. Regarding the center line, the unit tangential vector t, the unit normal vector n and the unit binormal vector b are defined, where $b = t \times n$ (see Figure 1b). The curvilinear coordinates (z, r, θ) (Germano [15]) are engaged is shown in Figure 1b. Here, z is the coordinate along the center line of the helical pipe in the direction of t, r is the radial coordinate and θ is the circumferential angle in a cross section of the pipe.

Simulations were performed for the non-dimensional curvature, $\delta = \frac{a}{R_h} = aR/(h^2 + R^2) = 0.01, 0.05, 0.1, 0.2$, 0.4 and the torsion parameter, $\beta = \tau/\sqrt{2\delta}$ as introduced by Kao [16] for a range of Reynolds number, *Re*, where R_h is the center line radius of curvature and $\tau = ah/(h^2 + R^2)$ is the non-dimensional torsion. Five types of helical pipe considered with the curvature for associating the outcome of the existing

simulation with the former studies [2-3]. Note that Datta et al. [9] executed the few outcomes for $\delta = 0.05, 0.1$.

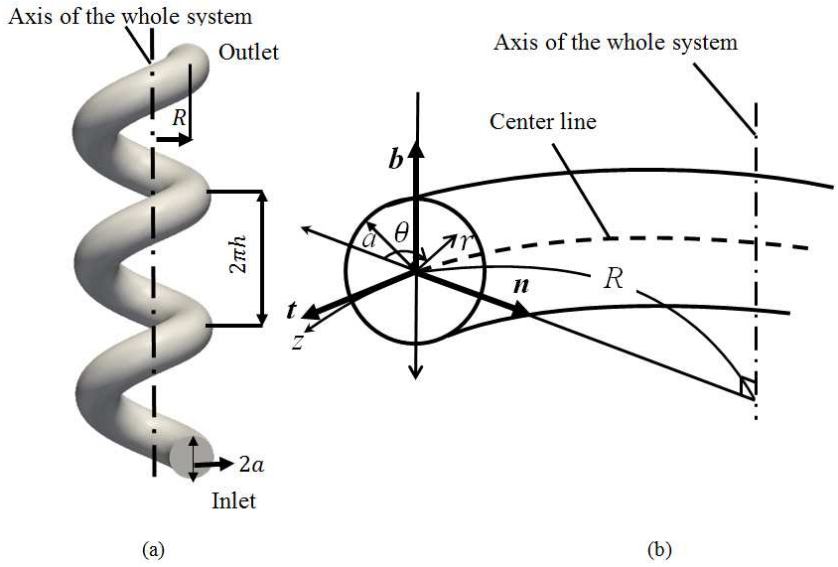

Figure 1. *(a) Helical pipe with circular cross section, (b) coordinate system.*

2.2. Governing Equations

The basic equations governing the flow are the viscous incompressible form of the continuity and Navier–Stokes equations:

$$\nabla \cdot U = 0, \tag{1}$$

$$\frac{\partial U}{\partial t} + (U \cdot \nabla)U = -\frac{1}{\rho}\nabla p + \nu \nabla^2 U, \tag{2}$$

where U is the velocity vector, t the time, p the pressure, ν the kinematic viscosity and ρ the density. Non-dimensional parameters: the Reynolds number, Re, and the Dean number, Dn, are defined by

$$Re = \frac{2a\,\bar{w}}{\nu}, Dn = Re\sqrt{\delta} \tag{3}$$

where $\bar{w}$ is the mean axial velocity, and ν is the kinematic viscosity.

Introduce a polar angle $(\theta + \varphi)$. Here, the angle φ is defined by

$$\varphi(z) = \int_{z_0'}^{z} \tau dz \tag{4}$$

z_0' be the arbitrary as long as $z \geq z_0'$

The governing equations in a helical pipe flow are written in the form of orthogonal curvilinear coordinates system as

$$\omega\frac{\partial u}{\partial z} + \frac{\partial v}{\partial r} + \frac{1}{r}\frac{\partial w}{\partial \theta} + \frac{v}{r} + \delta\omega[vsin(\theta+\varphi) + wcos(\theta+\varphi)] = 0 \tag{5}$$

$$Du + \delta u[vsin(\theta+\varphi) + wcos(\theta+\varphi)] = -\omega\frac{\partial p}{\partial z} + \frac{1}{Re}\left[\left(\frac{\partial}{\partial r} + \frac{1}{r}\right)\left(\frac{\partial u}{\partial r} + \delta\omega u\, sin(\theta+\varphi) - \omega\frac{\partial v}{\partial z}\right) + \frac{1}{r}\frac{\partial}{\partial\theta}\left(\frac{1}{r}\frac{\partial u}{\partial\theta}\right) + \delta\omega u cos(\theta+\varphi) - \omega\frac{\partial w}{\partial z}\right] \tag{6}$$

$$Dv - \frac{w^2}{r} - \delta\omega u^2 sin(\theta+\varphi) = \frac{\partial p}{\partial r} - \frac{1}{Re}\left[\left(\frac{\partial w}{\partial r} + \frac{w}{r} - \frac{1}{r}\frac{\partial v}{\partial\theta}\right)\left(\frac{1}{r}\frac{\partial}{\partial\theta} + \delta\omega\, cos(\theta+\varphi) - \omega\frac{\partial v}{\partial z}\right) - \omega\frac{\partial}{\partial z}\left(\omega\frac{\partial v}{\partial z} - \frac{\partial u}{\partial r} - \delta\omega u\, sin(\theta+\varphi)\right)\right] \tag{7}$$

$$Dw - \frac{vw}{r} - \delta\omega u^2 cos(\theta+\varphi) = -\frac{1}{r}\frac{\partial p}{\partial\theta} + \frac{1}{Re}\left[\left(\frac{\partial w}{\partial r} + \frac{w}{r} - \frac{1}{r}\frac{\partial v}{\partial\theta}\right)\left(\frac{\partial}{\partial r} + \delta\omega\, sin(\theta+\varphi)\right) - \omega\frac{\partial}{\partial z}\left(\frac{1}{r}\frac{\partial}{\partial\theta} - \omega\frac{\partial w}{\partial z} - \delta\omega u\, cos(\theta+\varphi)\right)\right] \tag{8}$$

where ω and D are defined by

$$D = \omega u\frac{\partial}{\partial z} + v\frac{\partial}{\partial r} + \frac{w}{r}\frac{\partial}{\partial\theta}$$

$$\omega = \frac{1}{1+\delta r sin(\theta+\varphi)}$$

2.3. Method of Numerical Simulation

By the direct numerical simulations to solve for the laminar, steady, incompressible flow upstream to downstream of helical pipe. Equations (1) and (2) are solved using the open-source computational fluid dynamics package OpenFOAM [17], and the simpleFoam solver, which implements the SIMPLE algorithm [18]. The cross sectional proper mesh in the r-θ plane of the domain was generated by OpenFoam, where the number of mesh in the radial direction is M, that in the circumferential direction N. The uniform mesh was generated in the z-direction, where the number of mesh is L.

Numerical solutions of the fluid motions require inflow and outflow boundary conditions for the pressure and velocity fields. For an inflow boundary condition, imposed a uniform axial flow resolved by the Reynolds number for the velocity and the gradient of pressure normal to the wall is zero. Zero normal gradient for the velocity and a fixed value for the pressure were imposed as an outflow boundary condition. No-

slip boundary condition was imposed on the wall.

2.4. Friction Factor

The friction factor of the pipe, f, is defined by

$$f = \frac{\Delta p}{L}\frac{2a}{\rho \overline{w}^2}, \tag{9}$$

where Δp is the pressure difference between two positions of the pipe in the region where the flow is well developed and axially invariant, and the distance between the two positions is L.

3. Results

By way of the cell-centered finite volume method (FVM) without turbulence model (DNS), three-dimensional steady calculations have been investigated for an extensive range of torsion parameters, and curvatures with the wide range of Reynolds numbers. In the present paper, considered five types of helical pipe. In this section, the outcomes of the friction factor of the axial direction in the well-developed region of the helical pipe are compared with the experimental data [3]. Then, in the steady calculations, the axial flow distribution have been illustrated due to the influence of torsion parameter. Finally, the friction factor for several types of helical pipe is comprehensively examined using parametric analysis.

3.1. Comparison with Experimental Data for $\delta = 0.01$

Due to the influence of β, the secondary flow of helical pipe makes different flow patterns from a toroidal pipe. When β is rationally close to zero (toroidal pipe), then symmetric two-cell vortex appears [12, 14], it's destroyed as β progressively increases. For enormous β, there is no significance of secondary flow, which is similar to the appearance of straight pipe. It should be noted that since torsion works as a rotational force, its effect is to induce a swirling motion in the pipe flow. Pattern variation of secondary flow shows a vital role because it describes the circumstances about the toroidal and helical pipe fluid flow explicitly. It is to be noted that same code used [8-10, 14] for conducting the present numerical calculations.

For authentication of the present DNS results, performed the numerical calculations for β = 0.50, 0.93, 1.19, 1.57, and 1.72, which has been confirmed with the experimental data [3]. Note that, performed $\delta = 0.01$ in the numerical calculations because the experimental curvature is rationally adjacent to 0.01. There is no experimental data for $\delta = 0.2, 0.4$. Also, compared the outcomes of the present DNS with Ito's correlation that's effective for toroidal pipe, as shown in Eq. 10 [19].

$$f_I = \frac{1376\sqrt{\delta}}{\left(1.56+\log_{10} Re\sqrt{\delta}\right)^{5.73}} \tag{10}$$

For assessment, depicted the present DNS results (○), the experimental data [3] (□), Eq. (10) (dotted line), Eq. (11) (dash-dotted line) as shown in Figures 2-6. The friction factor, f_s, of straight pipe for the laminar flow is described in Eq. [11].

$$f_s = \frac{64}{Re} \tag{11}$$

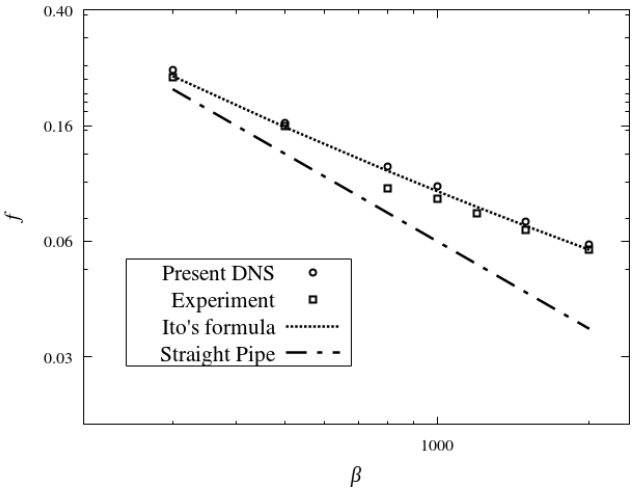

Figure 2. *Friction factor of the helical pipe for β = 0.5 and δ = 0.01.*

Figure 2 displays the friction factor of the helical pipe in the well-developed flow region by 3D DNS where the present results compared with the experimental data and conventional correlations for a toroidal pipe as a purpose of Reynolds number; thus, in addition to the Hagen-Poiseuille resistance formula for the straight pipe. In Figure 2, found that the friction factors obtained by present DNS agrees very well to the experimental data and rationally adjacent to Eq. (10) The trend of the friction factor by DNS is advanced than that of a toroidal pipe for small β. It is seen that at Reynolds numbers lower than 1800, the present DNS results and the experiment data coincide. At larger Reynolds number, the agreement is only reasonably good due to the laminar-turbulent transition effect. The critical Reynolds number of the laminar to turbulent transition investigated experimentally [3] and numerically [4] for $\delta = 0.01$ by observing the unsteady manners of the secondary and axial flows, where they found good agreement.

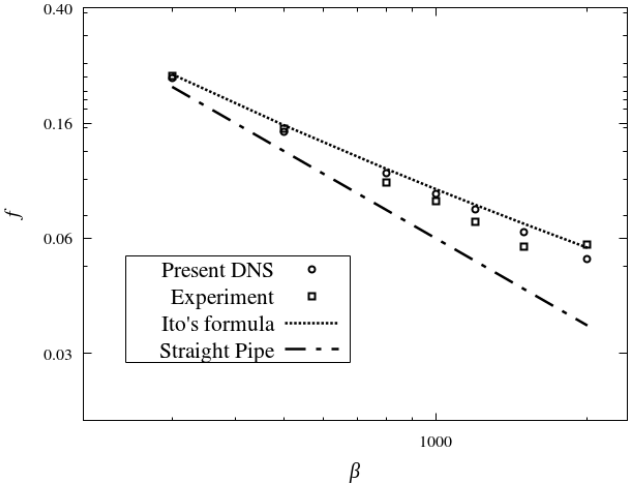

Figure 3. *Friction factor of the helical pipe for β = 0.93 and δ = 0.01.*

Figure 3 shows the present DNS results and experimental data consist below the curve of Eq. (10). It is evidently seen from Figure 3 that the friction factor of the toroidal pipe lies upstairs of the straight pipe. It is found that obtained the tendency of the friction factor of the helical pipe decreases as β increases, which is very adjacent to the experimental result and the agreement is in rationally good with the experimental data in the case of $\beta = 0.93$ due to the effect of turbulence as shown in Figure 3.

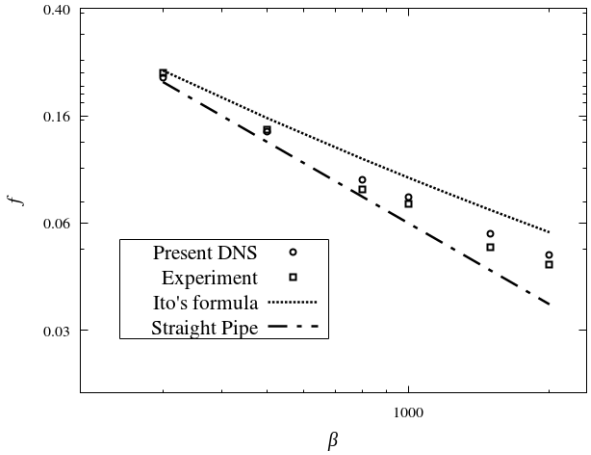

Figure 4. *Friction factor of the helical pipe for* $\beta = 1.19$ *and* $\delta = 0.01$.

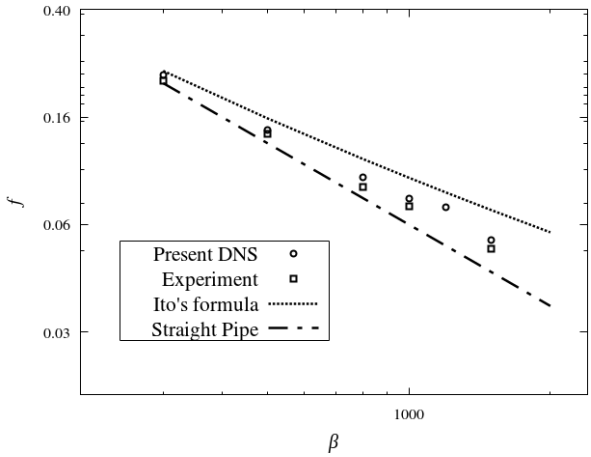

Figure 5. *Friction factor of the helical pipe for* $\beta = 1.52$ *and* $\delta = 0.01$.

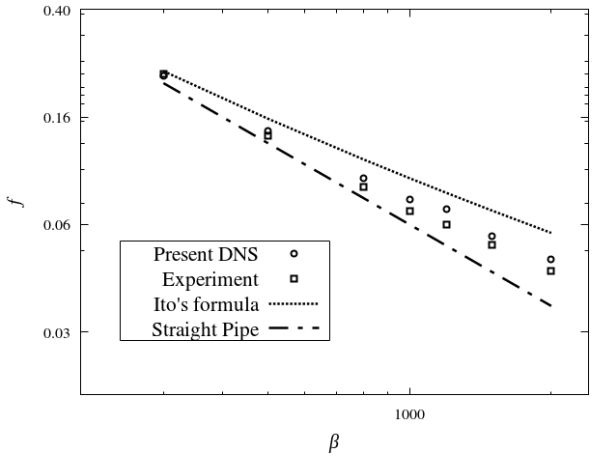

Figure 6. *Friction factor of the helical pipe for* $\beta = 1.72$ *and* $\delta = 0.01$.

In the numerical approach of the results of friction factor by DNS is in rationally good agreement with the experimental data, as shown in Figure 4. In Figure 4 depicted the trend of the friction factor as a role of the Reynolds number that indicates the appearance of the friction factor of the helical pipe is reduced, due to the swirl motion of the fluid by pitch induced torsion for constant centrifugal force due to curvature. As β increases. swirl motion of the fluid increases As a consequence, say that influences of torsion on the friction factor has more significant.

It can be clearly seen from Figures 5 and 6 that the friction factor of the helical pipe decreases as β increases and attain to the approach of the straight pipe if further β increases. It is interesting that, characteristics of the helical pipe are described using the finite value of β. The overall comparison of the results shows rather good accordance between the numerical and experimental results. As a consequence, from Figures 2-6, found that for small β cases, the friction factor of the helical pipe lies above the toroidal pipe. It is worth emphasizing that the friction factor of the helical pipe moderately decreases and approaches to the Hagen-Poiseuille flow as β increases to over 0.9. Note that the friction factor is inversely proportioned to the average flow velocity. Therefore, the influence of torsion on the helical pipe's friction factor becomes noticeable if β exceeds about 0.9 for $\delta = 0.01$, which is good agreement with the former study [3].

3.2. Axial Flow Distribution for $\delta = 0.01$

In the present 3D steady calculations, found the well-developed flow region. The axial flow does not change appreciably in the stream-wise direction in the well-developed flow region, which is in good agreement with those computed 3D DNS [14]. Secondary flow in a helical pipe is hardly affected by the influence of torsion where stream-wise flow is intensely reliant on it Therefore, it is vital to observe the distribution of the stream-wise flow in the helical pipe due to the influence of torsion and constant centrifugal force due to curvature.

In order to the study the axial flow distribution in a helical pipe due to the influence of torsion, depicted the axial velocity over the cross-section along the x-axis for $Re = 500$ at the well-developed flow region for an extensive range of β, $0.5 \leq \beta \leq 1.72$ for $Re = 500$, $\delta = 0.01$ in Figure 7, where x is nondimensionalized by dividing a and the axial velocity w is nondimensionalized by dividing by $\overline{w}$.

One of the key appearances of a helical pipe is that the curvature and stream-wise velocity induce the centrifugal force and the unevenness in the centrifugal force on a cross-section causes a secondary flow. The fluid located near the inner wall is moved toward the outer wall through the core region using disparity in the centrifugal force. A typical secondary flow is formed as a two-vortex pattern, where one appears near the top wall and the other near the bottom wall. If the influence of torsion appears, two-vortex pattern deviates into a single vortex pattern. It is

evidently that the torsion parameter effect is most prominent and the single-vortex pattern marked the axial velocity similar to the straight circular pipe for the laminar flow.

It is evidently seen in Figure 7, the position of the highest axial velocity consists adjacent the outer wall of the pipe for $\beta = 0.50$. It is interesting that, the position of the highest stream-wise velocity shifted near the inner wall of the helical pipe for $\beta = 0.93$. If β further rises, the position of highest axial velocity shifts away from the inner wall to the center of the cross-section of the helical pipe. For enormous β, axial velocity distribution attains a similar appearance of the straight pipe. It should be pointed out that the axial velocity rapidly increases from the inner to an outer wall along the x-axis for $\beta \leq 1.19$ on the cross section, whereas it becomes maximum for $\beta \cong 1.19$, as depcited in Figure 7. If β still larger, the maximum axial velocity gradually decreases.

As a consequence, say that the position of the highest stream-wise velocity turns around to the opposite direction of the swirl motion due to torsion for large β. When the value of β enormous, the stream-wise velocity may become very adjacent to the Hagen-Poiseuille flow.

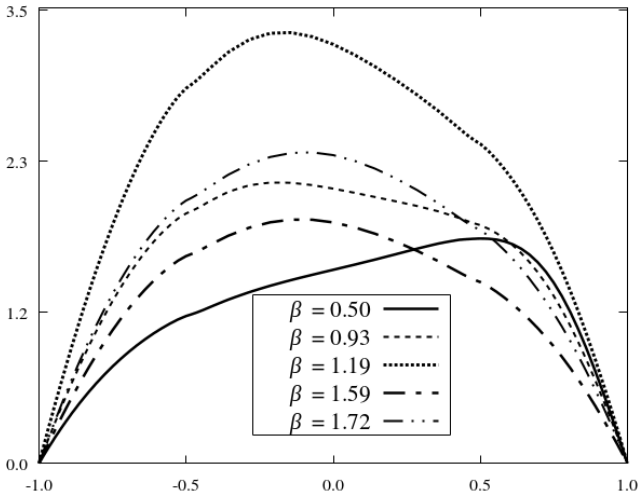

Figure 7. *Distribution of the axial velocity for* $0.5 \leq \beta \leq 1.72$ *and Re = 500 at* $\delta = 0.01$ *on the center line (y = 0).*

3.3. Friction Factor over a Wide Range of β

The validity of the foregoing analysis is amply demonstrated in Figures 8-10, where obtained friction factor behavior by present DNS is adequately described for an extensive range of β, $0.02 \leq \beta \leq 2.8$ and several Reynolds numbers. With this aim in mind, conducted five types of curvature, $\delta = 0.01, 0.05, 0.1, 0.2$ and 0.4 for describing the more evidently characteristics of the friction factor, where observed for $\delta = 0.05, 0.1$ by Datta et al. [14]. Note that, the present paper have no available experimental data for $\delta = 0.2$ and 0.4. In Figures 8-12, the friction factor of the helical pipe experimentally performed by Yamamoto et al. [3] is plotted as squares (■) and that obtained by the present 3D DNS is plotted as a circle (●). Equations (10) and (11) are also plotted in the figures.

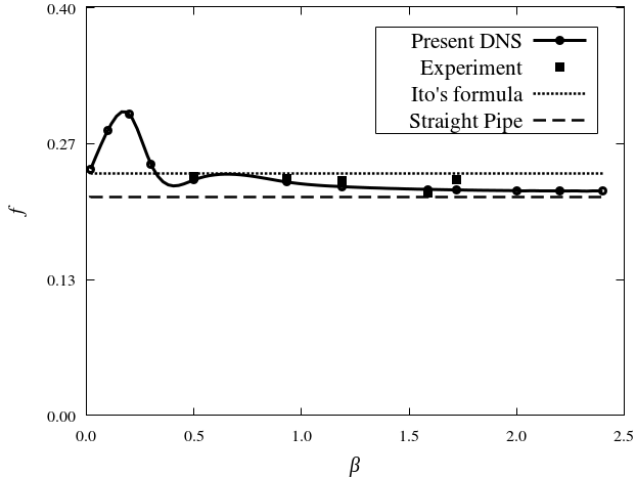

Figure 8. *Friction factor of the helical pipe for Re = 300 at* $\delta = 0.01$.

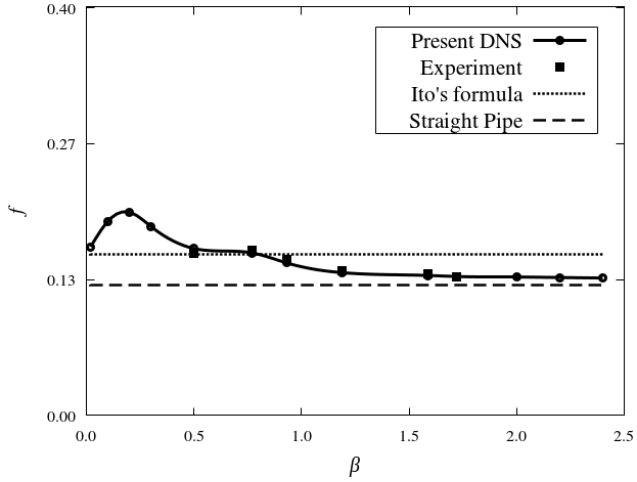

Figure 9. *Friction factor of the helical pipe for Re = 500 at* $\delta = 0.01$.

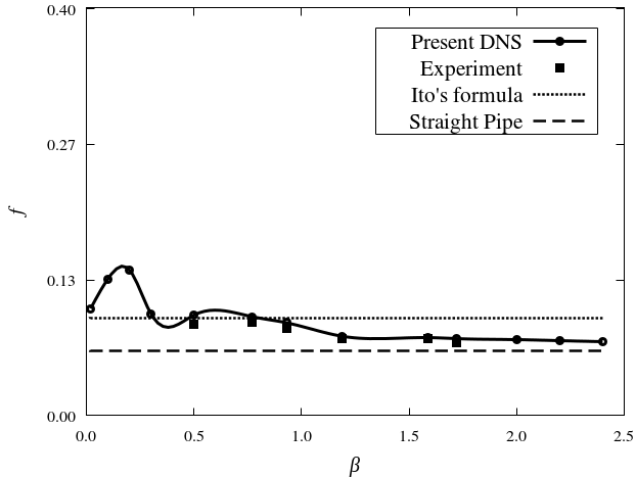

Figure 10. *Friction factor of the helical pipe for Re = 1000 at* $\delta = 0.01$.

In order to describe the physical mechanism of the friction factor of the helical pipe owing to the influence of β, displayed the friction factor of the helical pipe by present DNS with the experimental data [3] for several values of

Reynolds numbers. The comparison of the numerical friction factors with the predictive correlation and the experimental data are presented in Figures 8-10. One can observe from this figure that numerical results agree very well with correlated ones the predictive experimental data for Re = 300, 500, and 1000 at δ = 0.01, the exactness of the present numerical simulations is secured.

It should be pointed out that friction factor of the helical pipe rationally adjacent to the toroidal pipe for low torsion parameter ($\beta \cong 0.0$). If β increases from zero, friction factor of the helical pipe gradually increase from that of a toroidal pipe and attain to highest peak value, however, friction factor of the helical pipe deviates from the toroidal pipe. The torsion parameter, β, works as a rotational forces and found to play a vital role on the friction factor of the helical pipe. If β further increases, friction factor of the helical pipe almost monotonically decreases and approaches that of a straight pipe, which is good agreement with the former studies [14]. For an extensive range of β, observed that influence of torsion is most remarkable on the friction factor of the helical pipe whatever the curvature and the Reynolds Number in the laminar region. The highest peak of the friction factor occurs at $\beta \cong 0.3$, whatever the Reynolds number.

It is worth mentioning here that friction factor of the helical pipe by present DNS are in qualitatively agreement with those the computational study [2]. It is to be noted that the relative increase highest peak value of friction factor that lies in $\beta \cong 0.3$ from that a toroidal pipe by observing the friction factor for Re = 1000 at $\delta = 0.01$ in Figure 10. It is found that the friction factor promptly reduces from the highest value and slowly tends to that of a straight pipe as β increases for Re =1000. It is noteworthy that Liu and Masliyah [2] found the extreme peak value of the friction factor and trend of the friction factor quietly different from the results of present DNS for Dn = 100 and $\delta = 0.01$, which resemble to $Re \cong 1000$ since $Dn = Re\sqrt{\delta}$. It is interesting that the highest peak value of torsion parameter for low Reynolds number obtained whatever the value of curvature. Comparison of the present DNS with the former study [2], found that the relative increase highest peak value of the friction factor by the present numerical approach is 6% higher than that of the previous study [2]. Regarding the appearance of the friction factor for a straight pipe, the tendency of the friction factor by 3D DNS much more slowly than that the results of Liu and Masliyah [2], which is good agreement by Datta et al. [14]. It should be pointed out that computation condition of the present DNS is 3D, where computed results is two-dimensional (2D) by Liu and Masliyah [2]. In order to the present DNS result shows good agreement with the experimental data, it is very plausible that our results are more perfect than that the results of Liu and Masliyah [2].

4. Friction Factor over the Extensive Range of δ

It should be remarked that there are no numerical results of the friction factor of the helical pipe due to the influence of enormous curvature on the author's knowledge of literature. Therefore, influence of curvature on the friction factor of the helical pipe for an extensive range of torsion parameter and Reynolds number were conducted by 3D DNS, which is the first findings to the author's knowledge.

In the comprehensive study, perform the friction factor of the helical pipe due to the combined effect of curvature, $0.01 \leq \delta \leq 0.4$ and torsion parameter, $0.02 \leq \beta \leq 2.8$ with the Reynolds number, as depicted in Figures 11 and 12. It is seen that the tendency of the friction factor gradually reduces with the rise of Reynolds number. It can be evidently seen from Figures 11-12 that highest peak value of the friction factor occurs at $0.2 \leq \beta \leq 0.3$ for an extensive range of curvature, $0.01 \leq \delta \leq 0.4$, whatever the values of Reynolds number.

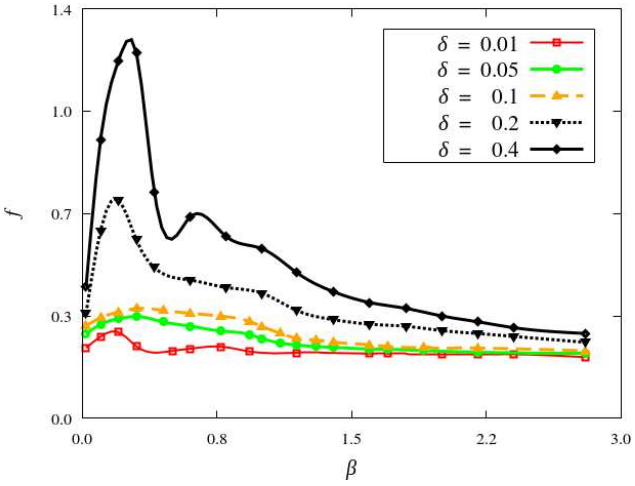

Figure 11. *Friction factor of the helical pipe for Re=300.*

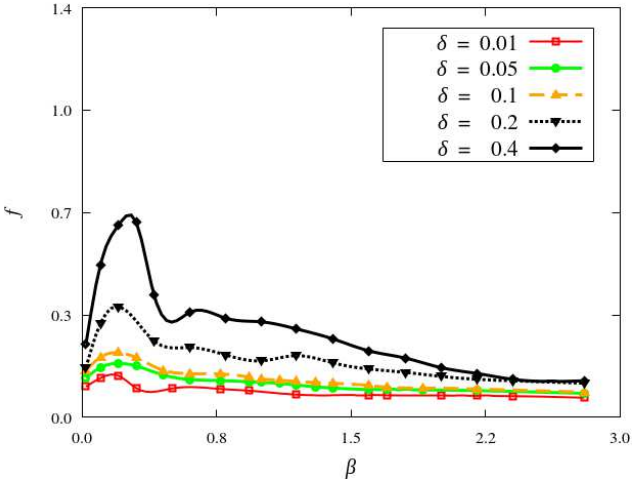

Figure 12. *Friction factor of the helical pipe for Re=1000.*

In the ongoing exploration, found that the friction factor formula of the toroidal pipe is appropriate for low torsion parameter cases. It is seen that friction factor of the helical pipe gradually increases from low β as β increases. If β further increases, friction factor decreases for $\beta >$ 0.3 at δ as depicted in Figures 11 and 12, respectively. It is to

be noted that the friction factor monotonically decreases from the peak value that deviates from a toroidal pipe and slowly approached to the straight pipe. It is interesting that the highest friction factor arises at $\beta \cong 0.3$, lies in the intermediate region over a wide range of β as illustrated by the three cases of Reynolds numbers in the existing paper, which are qualitatively resemble at $\delta = 0.1$ and 0.05. For the low Reynolds number (Figure 11), the peak of the friction factor is acute.

It should be remarked that the relative increase in the peak value from that for a toroidal pipe in the present DNS is slightly different by Liu and Masliyah. Liu and Masliyah [2] performed the friction factor of the helical pipe by the 2D numerical approach for Dn = 300 and $\delta = 0.16$ which resemble to $Re \cong 250$ since $Dn = Re\sqrt{\delta}$, qualitatively agree with the present results by 3D DNS for Re =300 at $\delta = 0.2$. It is worth mentioning that the highest peak of the friction factor by the present numerical is 6% higher than that of Liu and Masliyah [2], access of the present value much more slowly than that observed [2].

Trend of the friction factor of the helical pipe in the well-developed flow region shows approximately similar with global peak value due to the effect curvature. As Re increases, friction factor of the helical pipe decreases for every stage of curvature, as shown in Figures 11 and 12. It is found that relative increase of the peak value and magnitude of the friction factor increases if δ increases. From the discussion on Figures 8-12, conclude that the convenient correlation of the friction factor for a toroidal pipe is not appropriate to the helical pipe for $\beta \geq 0.05$ at $\delta = 0.01, 0.2, 0.4$ and $\beta \geq 0.1$ for $\delta = 0.1,$ and 0.05 [15]. To observed that the friction factor of the helical pipe approaches that of the straight pipe for $\beta > 2.5$ for low to higher Reynolds number.

5. Conclusion

A comprehensive numerical study of the viscous incompressible fluid flow through helical pipe with circular cross section has been conducted by the present 3D DNS and the friction factor of the helical pipe was obtained. OpenFOAM was used as a basic tool solve the Navier stokes equation without turbulence. To well explain the appearance of the friction factor of the helical pipe, obtained results were compared with the former study [2-3] for an extensive range of curvature, $0.01 \leq \delta \leq 0.4$; torsion parameter, $0.02 \leq \beta \leq 2.8$ and the Reynolds numbers.

Tendency of the friction factor of the helical pipe becomes higher than that of a toroidal pipe for low β, and the topologically deviates from that of a toroidal pipe if β further increases and attained in a straight pipe where curvature is changing from 0.01 to 0.4. Based on the experimental data, the influence of torsion on the friction factor of the helical pipe turn into enormous when $\beta \cong 0.9$ for $\delta = 0.01$, $\beta \cong 1.0$ for $\delta = 0.05$ and 0.1, and obtained the magnitude of the stream-wise velocity on well-developed cross sectional flow region. It should be pointed out that the position of the maximum stream-velocity moved from the horizontal line by the counter-rotating direction, whereas lies in the left-right upper part and center of the cross section as β increases from zero. By the ongoing investigation of the combine influences of curvature and torsion parameter on the friction factor, also found the parallel trend of the friction factor and growth of the friction factor upturn as curvature rises owing to the centrifugal force and swirl motion.

Obtained friction factors by 3D DNS are rationally agreement with the former studies based on the experimental [3] and 2D computational study [2] for an extensive range of curvature except the relative highest peak value of the friction factor and movement to the straight pipe if β gradually increases. It is interesting that found the highest peak of the friction factor for low to high curvature with the Reynolds number. Note that, Liu and Masliyah [2] didn't found the maximum peak of the friction factor for low Reynolds number. However, peak of the friction factor 6-7% larger than that of the result [2] In addition, found the friction factor of the helical pipe by the present DNS that's slowly approaching a straight pipe rather than the former study [2]. Since the present numerical approach was 3D and set up the boundary condition in the present DNS based on the experimental data, while the computational study [2] was 2D, so, our outcomes are assumed to be superior to those of the computational study [2].

It is worth emphasizing that the global maximum peak occurs in the range of $0.2 \leq \beta \leq 0.3$ whatever the comprehensive Reynolds number and curvature considered in the existing study; thus, the influence of torsion parameter and curvature establish a vital role in the helical. It is specified the applicable range of torsion parameters, $\beta \leq 0.05$, where appropriate the convenient correlation for the helical pipe with a zero pitch as demonstrated in this comprehensive study. In the parametric analysis, also specified the range of torsion parameters, $\beta > 2.5$, where the friction factor of straight pipe and helical pipe nearly adjacent. The fragmentary analysis reveals the influence of curvature and torsion on the friction factor that also afford the clarification about the chemical process along with the roughness of the helical pipe. So, the existing study may provide enhancement energy which is an innovative area in fluids engineering that is beneficial for pipe base applications.

Acknowledgements

A. K. Datta would like to acknowledge gratefully the financial support from University Grant Commission (UGC) for conduct this research work under the special allocation of 2018-2019.

References

[1] Yanase S., Goto N., Yamamoto K. Dual solutions of the flow through a curved tube. *Fluid Dyn. Res.* 1989; 5 (3): 191-201.

[2] Liu S., Masliyah J. H. Axially invariant laminar flow in helical pipes with a finite pitch. *J. Fluid Mech.* 1993; 251: 315-353.

[3] Yamamoto K., Akita T., Ikeuchi H., Kita Y. Experimental study of the flow in a helical circular tube. *Fluid Dyn. Res.* 1995; 16 (4): 237-249.

[4] Yamamoto K., Yanase S., Jiang R. Stability of the flow in a helical tube. *Fluid Dyn Res.* 1998; 22 (3): 153-170.

[5] Cioncolini A., Santini L. An experimental investigation regarding the laminar to turbulent flow transition in helically coiled pipes. *Exp. Therm. Fluid Sci.* 2006; 30: 367-380.

[6] Xiao Y., Hu Z., Chen S., Gu H. Experimental study of two-phase frictional pressure drop of steam-water in helically coiled tubes with small coil diameters at high pressure. *Appl. Therm. Eng.* 2018; 132: 18–29.

[7] Yu J., Jiang Y., Cai W., Li X., Zhu Z. Condensation flow patterns and heat transfer correction for zeotropic hydrocarbon mixtures in a helically coiled tube. *Int. J. Heat Mass Tran.* 2019; 143: 118500.

[8] Datta AK., Hayamizu Y., Kouchi T., Nagata Y., Yamamoto K., Yanase S. Numerical study of turbulent helical pipe flow with comparison to the experimental. *J. Fluid Eng.* 2017; 139 (9): 091204.

[9] Datta AK., Yanase S., Hayamizu Y., Kouchi T., Nagata Y., Yamamoto K. Effect of torsion on the friction factor of helical pipe flow. *J. Phys. Soc. Japan* 2017; 86: 064403.

[10] Datta AK., Yanase S., Hayamizu Y., Kouchi T., Shatat MME. Laminar forced convective heat transfer in helical pipe flow. *Int. J. Thermal Sci.* 2017; 120; 41-49.

[11] Garcia JP., Garcia A., Martin RH, Solano JP. Experimental correlations on critical Reynolds numbers and friction factor in tubes with wire-coil inserts in laminar, transitional and low turbulent flow regimes. *Exp. Therm. Fluid Sci.* 2018; 91: 64-79.

[12] R. H. Patil, Fluid flow and heat transfer analogy for laminar and turbulent flow inside spiral tubes. Int. J. Thermal Sci. 139 (2019) 362-375.

[13] Solanki AK., Kumar R. Condensation frictional pressure drop characteristic of R-600a inside the horizontal smooth and dimpled helical coiled tube in shell type heat exchanger. *Int. J. Thermal Sci.* 2020; 154: 106406.

[14] Datta AK., Kouchi T., Hayamizu Y., Nagata Y., Yamamoto K., Yanase S. Existence of dual solutions and three-dimensional instability of helical pipe flow. *Chinese J. Phys.* 2021; 73: 154-166.

[15] Germano M. On the effect of torsion on a helical pipe flow. *J. Fluid Mech.* 1982; 125: 1-8.

[16] Kao HC. Torsion effect on fully developed flow in a helical pipe. *J. Fluid Mech.* 1987; 184: 335-356.

[17] OpenFOAM. The open source cfd toolkit: User guide 2014. https://openfoam.org.

[18] Patankar SV., Spalding DB. A Calculation Procedure for Heat, Mass and Momentum Transfer in Three-Dimensional Parabolic Flows. *Int. J. Heat Mass Transfer* 1972; 15 (10): 1787–1806.

[19] Ito H. Friction factor for turbulent flow in curved pipe. *J. Basic Eng. Trans. ASME D* 1959; 81: 123-134.